Acta Biomaterialia 42 (2016) 46–55

Contents lists available at ScienceDirect

Acta Biomaterialia

journal homepage: www.elsevier.com/locate/actabiomat

Full length article

Matrix directed adipogenesis and neurogenesis of mesenchymal stem cells derived from adipose tissue and bone marrow

Junmin Lee [a,b], Amr A. Abdeen [a,b], Xin Tang [b,c,1], Taher A. Saif [b,c], Kristopher A. Kilian [a,b,*]

[a] Department of Materials Science and Engineering, University of Illinois at Urbana-Champaign, Urbana, IL 61801, USA
[b] Micro and Nanotechnology Laboratory, University of Illinois at Urbana-Champaign, Urbana, IL 61801, USA
[c] Department of Mechanical Science and Engineering, University of Illinois at Urbana-Champaign, Urbana, IL 61801, USA

ARTICLE INFO

Article history:
Received 12 February 2016
Received in revised form 14 June 2016
Accepted 28 June 2016
Available online 29 June 2016

Keywords:
Mesenchymal stem cells
Bone marrow
Adipose derived
Differentiation
Microenvironment

ABSTRACT

Mesenchymal stem cells (MSCs) can differentiate into multiple lineages through guidance from the biophysical and biochemical properties of the extracellular matrix. In this work we conduct a combinatorial study of matrix properties that influence adipogenesis and neurogenesis including: adhesion proteins, stiffness, and cell geometry, for mesenchymal stem cells derived from adipose tissue (AT-MSCs) and bone marrow (BM-MSCs). We uncover distinct differences in integrin expression, the magnitude of traction stress, and lineage specification to adipocytes and neuron-like cells between cell sources. In the absence of media supplements, adipogenesis in AT-MSCs is not significantly influenced by matrix properties, while the converse is true in BM-MSCs. Both cell types show changes in the expression of neurogenesis markers as matrix cues are varied. When cultured on laminin conjugated microislands of the same adhesive area, BM-MSCs display elevated adipogenesis markers, while AT-MSCs display elevated neurogenesis markers; integrin analysis suggests neurogenesis in AT-MSCs is guided by adhesion through integrin $\alpha_v\beta_3$. Overall, the properties of the extracellular matrix guides MSC adhesion and lineage specification to different degrees and outcomes, in spite of their similarities in general characteristics. This work will help guide the selection of MSCs and matrix components for applications where high fidelity of differentiation outcome is desired.

Statement of Significance

Mesenchymal stem cells (MSCs) are an attractive cell type for stem cell therapies; however, in order for these cells to be useful in medicine, we need to understand how they respond to the physical and chemical environments of tissue. Here, we explore how two promising sources of MSCs—those derived from bone marrow and from adipose tissue—respond to the compliance and composition of tissue using model extracellular matrices. Our results demonstrate a source-specific propensity to undergo adipogenesis and neurogenesis, and uncover a role for adhesion, and the degree of traction force exerted on the substrate in guiding these lineage outcomes.

© 2016 Acta Materialia Inc. Published by Elsevier Ltd. All rights reserved.

1. Introduction

The interface between cells and materials is a dynamic and complex environment where cells in contact with materials can sense their properties such as stiffness, matrix protein, and geometry and respond to these cues in multiple ways including through mechanical forces exerted on the matrix by the cells [1]. Cells incorporate these cues via signal propagation through integrins, and eventually translate this information into regulation of gene expression and cell fate decisions [2]. Advances in biomaterials to direct stem cell lineage decisions have focused on designing biomimetic materials that realize the "in vivo" microenvironments' ability to interact with cells [3–5]. However, not only is designing tailored biomaterials that present multiple signals challenging, but the precise roles of physical and biochemical cues in coordinating cellular processes such as migration, proliferation, and differentiation remains difficult to dissect.

* Corresponding author at: Department of Materials Science and Engineering, University of Illinois at Urbana-Champaign, Urbana, IL 61801, USA.
E-mail address: kakilian@illinois.edu (K.A. Kilian).
[1] Present address: Department of Chemistry and Chemical Biology, Harvard University, Cambridge, MA 02138, USA.

http://dx.doi.org/10.1016/j.actbio.2016.06.037
1742-7061/© 2016 Acta Materialia Inc. Published by Elsevier Ltd. All rights reserved.

Mesenchymal stem cells (MSCs), traditionally isolated from the bone marrow (BM-MSC), have fibroblast-like morphology and are known to differ from other cell types such as endothelial cells and macrophages in terms of basic characteristics [6]. However, MSCs can also be isolated from other tissues ranging from skin to adipose tissues [7,8]. MSCs isolated from adipose tissues (AT-MSCs), for example, not only have greater proliferative potential compared to BM-MSCs, but are easier to harvest and more abundant, which has led to an increase in interest in their use [9]. Irrespective of cell source, MSCs display common expression of surface markers such as CD73, CD90, and CD105, while lacking the surface marker expression of CD11b, CD14, CD45, CD79a and HLA-DR [10]. Several studies have compared AT- and BM-MSCs in terms of immunophenotype [11,12], proliferation [8], differentiation [13], and gene expression [14], with some differences between source noted. For example, BM-MSCs show a higher capacity for osteogenic and chondrogenic differentiation than AT-MSCs [15,16] while AT-MSCs tend to possess higher levels of adipogenic differentiation potential [17,18].

In addition to the classical differentiation pathways of adipogenesis, chondrogenesis and osteogenesis [19], recent studies show that MSCs have the plasticity to differentiate into cells of ectodermic origin like neurocytes [20,21]. MSC lineage specification has been shown to be sensitive to biophysical and biochemical cues such as matrix stiffness, cell geometry, and adhesion ligands which exist in the surrounding microenvironment [22–27]. For instance, in a previous study we found that MSCs isolated from bone marrow can undergo both adipogenesis and neurogenesis on soft substrates (~0.5 kPa) [24]. Adipogenesis is believed to occur in two stages [28]. The first stage is commitment of MSCs to preadipocytic differentiation which can be regulated by biophysical and biochemical cues such as matrix elasticity [29], cell shape [23,30], and matrix ligand [24,26] while the second stage is terminal differentiation to mature adipocytes through activation of peroxisome proliferator-activated receptor-γ (PPAR γ) [28]. MSCs that adopt characteristics of neuronal cells [31,32], demonstrate high expression of neurogenic markers such as neuroepithelial stem cell intermediate filament (NESTIN), microtubule associated protein 2 (MAP2), and β3 tubulin [33–35]. Our previous study revealed cell spreading on soft substrates mimicking the modulus of brain tissues promotes elevated expression of neurogenic markers (β3 tubulin & MAP2) in the absence of chemical differentiation medium [24]. In contrast, MSCs cultured in confined geometries express higher levels of adipogenesis markers (PPAR γ and Lipoprotein lipase (LPL)). In addition, cells cultured on fibronectin conjugated matrices tend to express higher levels of adipogenic markers as opposed to those cultured on collagen coated substrates which show elevated expression of neurogenic markers.

MSCs are believed to regulate "stemness" or lineage choices through dynamic interactions with the ECM in vivo [36–41]. Integrins, combinations of two different chains (α and β subunits), are a class of cell-surface receptors which interact with the ECM [42] by binding to matrix proteins such as fibronectin, laminin, and collagen [43,44] and regulate cellular functions, including differentiation [2]. For example, we have previously shown that osteogenic differentiation of BM-MSCs cultured on 30 kPa substrates can be regulated through integrin $\alpha_5\beta_1$ [45]. Focal adhesions, which are integrin-containing multi-protein structures connecting the cell cytoskeleton to the ECM, play a crucial role in cell signaling by sensing and transducing dynamics of chemical and mechanical properties of the ECM [46]. Traction stress exerted on the ECM through focal adhesions is regarded as an important indicator for BM-MSC differentiation [47]. For example, traction forces exerted by MSCs cultured on soft substrates are low, resulting in adipogenic differentiation, while cells cultured on stiffer substrates exerted higher traction forces, leading to an osteogenic outcome [48].

In this paper, we show how controlling matrix elasticity, adhesive protein, and cell shape can be employed to study the comparative differentiation potential of MSCs isolated from different sources. Immunofluorescence staining is used to investigate the expression of key markers during adipogenesis and neurogenesis. We directly measure the stresses generated by cells under different combinations of matrix protein and cell shape. Multiple types of integrins expressed by MSCs are investigated to reveal the relation of specific integrins, traction stress, and differentiation potential.

2. Materials and methods

2.1. Materials

All materials including laboratory chemicals and reagents were purchased from Sigma unless otherwise noted. Tissue culture plastic (12 well plates) and glass coverslips (18 mm circular) were purchased from Fisher Scientific. Cell culture media and 0.25% trypsin were purchased from Gibco. Nile red was purchased from Fisher Scientific (N1142), Rabbit *anti*-PPAR γ was purchased from Cell Signaling (C26H12), Rabbit *anti*-paxillin (ab32084) and Chicken *anti*-MAP2 (ab5392) were purchased from Abcam Technologies, Mouse anti-β3 tubulin was purchased from Sigma (T8660), and Mouse anti-$\alpha_v\beta_3$ (MAB1976Z) was purchased from Millipore. 4,6-diamidino-2-phenylindole (DAPI), Alexa488-phalloidin, Tetramethylrhodamine-conjugated *anti*-rabbit IgG antibody, Alexa Fluor 647-conjugated *anti*-chicken IgG antibody, and Alexa Fluor 647-conjugated *anti*-mouse IgG antibody were purchased from Invitrogen.

2.2. Surface preparation

Polyacrylamide substrates were fabricated as previously described [49]. Briefly, desired stiffness (0.5–40 kPa) gels were made by using the mixture of Acrylamide and Bis-acrylamide as reported previously [50]. To initiate gelation, 0.1% of Ammonium Persulfate (APS) and Tetramethylethylenediamine (TEMED) were employed. After polymerization, gels were gently detached from hydrophobically-treated glass. We utilized hydrazine hydrate 55% (Fisher Scientific) for 2 h with rocking to modify the surface chemistry of gels from amide groups to more reactive hydrazide groups. 5% Glacial acetic acid for 1 h with rocking was used to rinse the hydrazine followed by distilled water for at least 1 h to rinse the acetic acid. To generate patterned surfaces, polydimethylsiloxane (PDMS, Polysciences, Inc.) stamps were made by polymerization upon a patterned master of photoresist (SU-8, MicroChem) fabricated using UV photolithography through a laser printed mask. 25 μg/ml of fibronectin, laminin or type I collagen (for combinations of proteins, the total final concentration was fixed at 25 μg/ml) in PBS were mixed with sodium periodate (~3.5 mg/ml) for at least 45 min to generate free aldehydes on matrix proteins. The protein solutions were pipetted onto patterned or non-patterned stamps for 30 min and then dried with air. Proteins were transferred from stamps to gel surfaces by micro-contact printing and chemically conjugated through the reaction between free aldehydes in proteins and reactive hydrazide groups on the gels. Patterned gels were rinsed at least three times before cell culture.

2.3. Cell source, culture, and integrin blocking assays

MSCs isolated from adipose tissues or bone marrow (AT- and BM-MSCs respectively) were purchased from Lonza and tested positive for CD29, CD44, CD105, and CD166 and negative for CD14, CD34, and CD45 by flow cytometry to verify stem cell characteristics (http://www.lonza.com). AT- and BM-MSCs were

cultured and then expanded. Cells were cryopreserved (10% DMSO) at passage 2 and thawed and cultured in Dulbecco's Modified Eagle's Medium (DMEM) low glucose (1 g/ml) media supplemented with 10% fetal bovine serum (FBS, Invitrogen), and 1% penicillin/streptomycin (P/S). Cells were passaged around 80–90% confluency and used for experiments at around passage 4–8 (~5000 cells/cm^2). Media was changed every 3 or 4 days and cells were fixed after culture for 10 days. For integrin blocking, antibodies ($\alpha_v\beta_3$) were added to cells in media before and after seeding and at each media change at 1 μg/ml. For the induction media experiments, adipogenic induction (high glucose DMEM containing FBS and P/S, Gentamicin/Amphotericin, L-glutamine, dexamethasone, indomethacin, 3-isobutyl-1-methylxanthine and insulin: days 1–3 and 6–8) and maintenance media (low glucose DMEM containing FBS and P/S, Gentamicin/Amphotericin, L-glutamine and insulin: days 4–5 and 9–10) and osteogenic induction medium (low glucose DMEM containing FBS and P/S, Gentamicin/Amphotericin, L-glutamine, dexamethasone, ascorbate and β-glycerophosphate: days 1–10) were purchased from Lonza. Neurogenic induction medium (low glucose DMEM supplemented with 5 mM β-mercaptoethanol: days 1–10) was employed as previously described [9].

2.4. Immunocytochemistry

Cells cultured on patterned or non-patterned surfaces for 10 days were fixed with 4% paraformaldehyde (Alfa Aesar) for 20 min. 0.1% Triton X-100 in PBS was used for 30 min to permeabilize cells and cells were blocked with 1% bovine serum albumin (BSA) for 15 min and then labeled with primary antibodies (PPAR γ, Paxillin, MAP2, or β3 tubulin) in 1% BSA in PBS (1:500 dilution) for 2 h at room temperature (~20 °C). Surfaces were rinsed three times and then secondary antibody labeling was conducted in 2% goat serum containing 1% BSA in PBS for 20 min in a humid incubator (5% CO_2 and 37 °C) with 4,6-diamidino-2-phenylindole (DAPI, 1:2500 dilution) for nuclear staining, Alexa488-phalloidin (1:200 dilution) for actin staining, Tetramethylrhodamine-conjugated *anti*-rabbit IgG antibody (1:200 dilution) for PPAR γ or Paxillin, Alexa Fluor 647-conjugated *anti*-chicken IgG antibody (1:200 dilution) for MAP2, and Alexa Fluor 647-conjugated *anti*-mouse IgG antibody (1:200 dilution) for β3 tubulin. Surfaces were rinsed three times and then mounted on a glass slide to conduct immunofluorescence microscopy by using a Zeiss Axiovert 200 M inverted research-grade microscope (Carl Zeiss, Inc.). ImageJ was employed to analyze immunofluorescence images by measuring average fluorescence intensity. For Nile red staining, after fixing cells, each sample was stained with Nile red (lipophilic stain). Briefly, cells were fixed with paraformaldehyde for 20 min followed by immersion in Nile red working solution (1 μg/ml Nile red in PBS) for 20 min at 4 °C. Nuclei were counterstained with DAPI.

2.5. Traction stress measurement

Traction stress measurements were performed as previously described [45] and the detailed procedures of cell traction computation using finite element methods can be found in a previous report [51]. Briefly, fluorescent bead-infused gels were obtained by mixing polyacrylamide solutions as described above with a 1 mm-bead suspension (Invitrogen, F-8821) at 1:250. Patterning of matrix proteins was performed as described above. An Olympus IX81 fluorescent microscope and 20× objective was employed to obtain live cell images (5% CO_2 and 37 °C). Firstly, bright field images were obtained for cells to visualize their shape and location, and then fluorescent bead images were taken. Next, cells were removed from the surface with sodium dodecyl sulfate (SDS, Fisher Inc.), and the gels relax to their initial state without cells, leading to accessing the displacement of beads under the null-force condition. The gel displacements were characterized via Matlab digital image correlation programs [51] using the images before and after cell removal (ux and uy). Since Fz = 0 for all surface nodes leads to an error of less than 2% in the force calculation of Fx and Fy, we did not measure uz during the experiments.

2.6. RNA isolation and RT-PCR

Adherent cells cultured for 1 day were lysed in TRIZOL reagent (Invitrogen). Total RNA was isolated using chloroform extraction and ethanol precipitation and reverse transcribed using Superscript III® First Strand Synthesis System for RT-PCR (Invitrogen). All reactions were performed linearly by cycle number for each set of primers using SYBR® Green Real-Time PCR Master Mix (Invitrogen) on an Eppendorf Realplex 4S Real-time PCR system. Primer sequences were as follows: α1 CTC CTCACTGTTGTTCTACGCT and ATCCAAACATGTCTTCCACCG, α3 CCCACCTGGTGTGACTTCTT and TCCCTGGAGGTGGGTAGC, α5 TGCCGAGTTCACCAAGACTG and TGCAATCTGCTCCTGAGTGG, αv CATCTTAATGTTGTGCCGGATGT and TCCTTCCACAATCCCAGGCT, α6 CAACTTGGACACTCGGGAGG and ACGAGCAACAGCCGCTT, β1 CCGCGCGGAAAAGATGAATTT and AGCAAACACACAGCAAACTGA, β3 TTGGAGACACGGTGAGCTTC and GCCCACGGGCTTTATGGTAA, GAPDH TGCCTCGATGGGTGGAGT and GCCCAATACGACCAAATCAGA.

2.7. Statistical analysis

Error bars represent standard deviation (SD) and data was obtained from 3 independent experiments unless otherwise specified. For statistical analysis, one-way ANOVA for comparing two groups or multiple groups were employed and values of $P < 0.05$ were considered statistically significant.

3. Results

3.1. The influence of matrix stiffness, geometry, and adhesion ligand on AT- and BM-MSCs differentiation

To explore the influence of physical and biochemical cues on AT- and BM-MSC differentiation we selected polyacrylamide hydrogels as they are inexpensive, easily and quickly tailored to exhibit a wide range of mechanical properties, biocompatible, and have an easy to modify surface chemistry for conjugating matrix proteins [49]. We fabricated polyacrylamide hydrogels with tunable matrix stiffness and microcontact printed islands of adhesive proteins (fibronectin, laminin, or collagen) with different geometries to study the effects of substrate elasticity, matrix composition and cell shape on controlling adipogenesis and neurogenesis of AT- and BM-MSCs. We used representative adipogenic (PPAR γ) and neurogenic (β3 tubulin) markers to compare the degree of early stage adipogenesis and neurogenesis specification. Polyacrylamide hydrogels with a range of stiffness (0.5–40 kPa) were prepared since this range of elasticity is physiologically relevant with around 0.5, 10 and 30 kPa spanning the rigidity of brain, muscle, and pre-calcified bone tissue, respectively [20]. First, we studied the morphology of cells cultured for 10 days on fibronectin coated hydrogels. Morphological analysis reveals that BM-MSCs cultured on non-patterned substrates present a variable cell spread area depending on substrate stiffness (0.5 kPa: 5000 μm^2 to 40 kPa: 15,000 μm^2) and AT-MSCs show the same trend with varying stiffness but with much smaller average areas (~2.4-fold smaller across the range 0.5–40 kPa) and with cells being more branched than BM-MSCs (Fig. 1a and b). Next, we investigated adipogenic and neurogenic marker expression of the two different

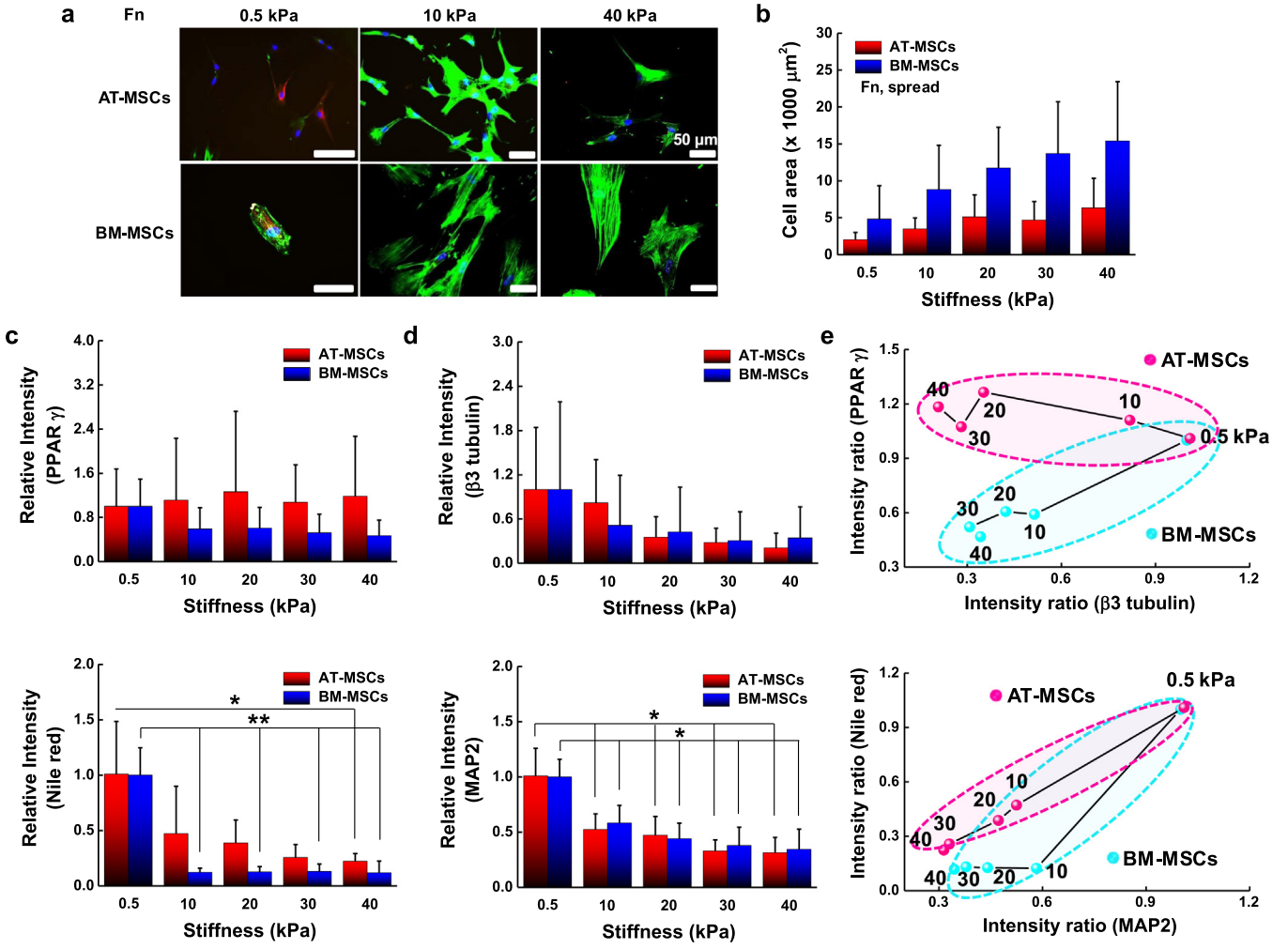

Fig. 1. AT-MSCs and BM-MSCs express markers associated with adipogenesis and neurogenesis in a stiffness dependent manner. (a) Representative merged immunofluorescence images of MSCs with nuclei (blue), actin (green), PPAR γ (yellow) and β3 tubulin (red). Scale bar: 50 μm. (b) Cell areas of at least 100 AT-MSCs and BM-MSCs cultured for 10 days on substrates of different stiffness. Expression of (c) adipogenic (PPAR γ and Nile red) and (d) neurogenic (β3 tubulin and MAP2) markers for those populations reveal how AT-MSCs and BM-MSCs express these markers differently in a stiffness dependent manner. (N = 3) (e) Plot of average values of marker expression with varying stiffness (x-axis: β3 tubulin/MAP2 and y-axis: PPAR γ/Nile red). Error bars represent s.d. (For interpretation of the references to colour in this figure legend, the reader is referred to the web version of this article.)

types of MSCs cultured for 10 days on non-patterned surfaces of fibronectin coated hydrogels (~0.5–40 kPa). AT- and BM-MSCs cultured on substrates with different stiffness expressed markers associated with adipogenesis and neurogenesis in a stiffness dependent manner. For PPAR γ expression, AT-MSCs show no significant changes with stiffness (~0.5–40 kPa), while BM-MSCs tend to express lower PPAR γ levels with increasing stiffness (Fig. 1c). For β3 tubulin expression, both AT- and BM-MSCs display decreased marker expression with increasing stiffness (Fig. 1d). Plotting average values of marker expression with varying stiffness (x-axis: β3 tubulin and y-axis: PPAR γ) (Fig. 1e), it is clear that while both MSC types show large changes in β3 tubulin expression with stiffness, adipogenic marker expression is only responsive to stiffness for BM-MSCs. Although the trend lines are not statistically significant for PPAR γ and β3 tubulin due to high variability in expression, possibly due to population heterogeneity as shown in previous studies [52], trend analysis was used to guide further mechanistic studies. To verify the results from the use of PPAR γ and β3 tubulin, we employed other adipogenic and neurogenic markers: Nile red (lipophilic stain) for adipogenesis and Microtubule-Associated Protein 2 (MAP2) for neurogenesis. The expression trend of MAP2 shows a decrease with increasing matrix elasticity and follows the results for β3 tubulin (Fig. 1d). For Nile red staining, both AT- and BM-MSCs cultured on soft substrates (0.5 kPa) show higher accumulation of lipid droplets compared to those cultured on stiffer substrates (Fig. 1c and Fig. S1). However, comparable to the results of PPAR γ expression, lipid accumulation is influenced less by stiffness in AT-MSCs than in BM-MSCs (Fig. 1e). To explore how cell shape differentially regulates adipogenesis and neurogenesis of AT- and BM-MSCs, we employed various geometries: circular shapes with different areas (1000, 3000, 5000 μm^2) or different aspect ratios (4:1 and 8:1) with a fixed area (3000 μm^2) on fibronectin coated hydrogels (~0.5 kPa, which approximates the stiffness of brain and fat tissue). In our previous study with BM-MSCs, increasing cell area or aspect ratio gave rise to decreased adipogenic and increased neurogenic differentiation [24]. AT- and BM-MSCs both follow this trend but with different sensitivities (Fig. 2a and b; the differences between neurogenesis and adipogenesis on 5000 μm^2 circle and 8:1 oval patterned substrates for AT-MSCs and 4:1 oval patterned substrates for BM-MSCs being statistically significant). Both AT- and BM-MSCs show decreased PPAR γ expression and increased β3 tubulin expression with increasing cell area (Fig. 2c). As with stiffness, AT-MSCs are much less prone to changes in PPAR γ expression than

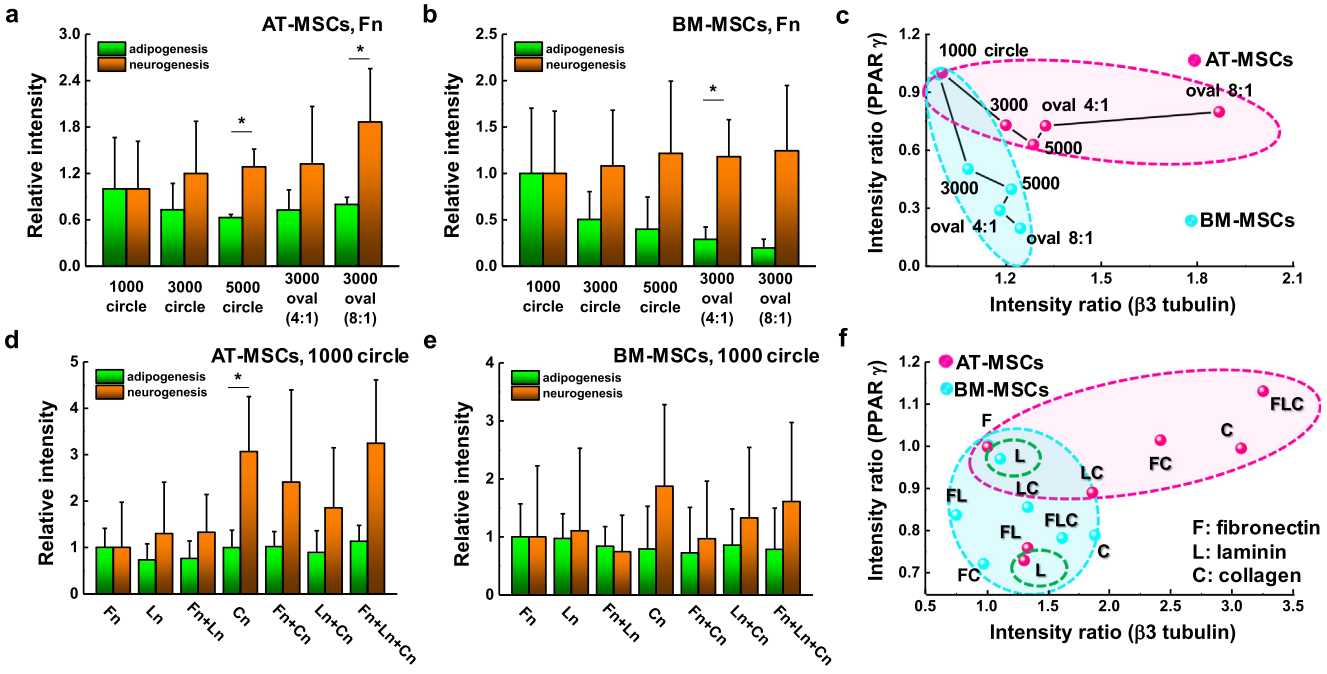

Fig. 2. AT-MSCs and BM-MSCs express markers associated with adipogenesis and neurogenesis in a geometry and matrix protein dependent manner. Expression of adipogenic (PPAR γ) and neurogenic (β3 tubulin) markers for (a) AT-MSCs and (b) BM-MSCs cultured on various single cell geometries. (N = 3) (c) Plot of average values of marker expressions with varying geometry (x-axis: β3 tubulin and y-axis: PPAR γ). Expression of PPAR γ and β3 tubulin markers for (d) AT-MSCs and (e) BM-MSCs cultured on different matrix proteins, individually and when mixed together on gel surfaces. (N = 3) (f) Plot of average values of marker expression with varying matrix protein (x-axis: β3 tubulin and y-axis: PPAR γ). (*P < 0.05, one-way ANOVA). Error bars represent s.d.

BM-MSCs. The opposite is true for β3 tubulin where changes in aspect ratio cause up to ~1.5-fold increase in expression with AT-MSCs while only causing a ~0.2-fold increase in BM-MSCs. These results would indicate that cell shape plays a bigger role for neurogenic differentiation of AT-MSCs than BM-MSCs with the opposite being true for adipogenic differentiation (BM-MSCs are more sensitive to shape changes).

Next, we patterned three different matrix proteins; fibronectin, laminin, and collagen, individually and when mixed together on the surface of gels to investigate the distinct effects of matrix protein on controlling different levels of adipogenesis and neurogenesis of AT- and BM-MSCs. As we previously reported for BM-MSCs [24], cells on fibronectin coated substrates (1000 μm^2 circle) express higher levels of adipogenic markers, while those on type I collagen patterned matrices (1000 μm^2 circle) tend to favor neurogenesis (Fig. 2d and e). AT-MSCs on collagen (alone or mixed with other proteins) coated substrates expressed much higher levels of β3 tubulin with almost no change in PPAR γ compared

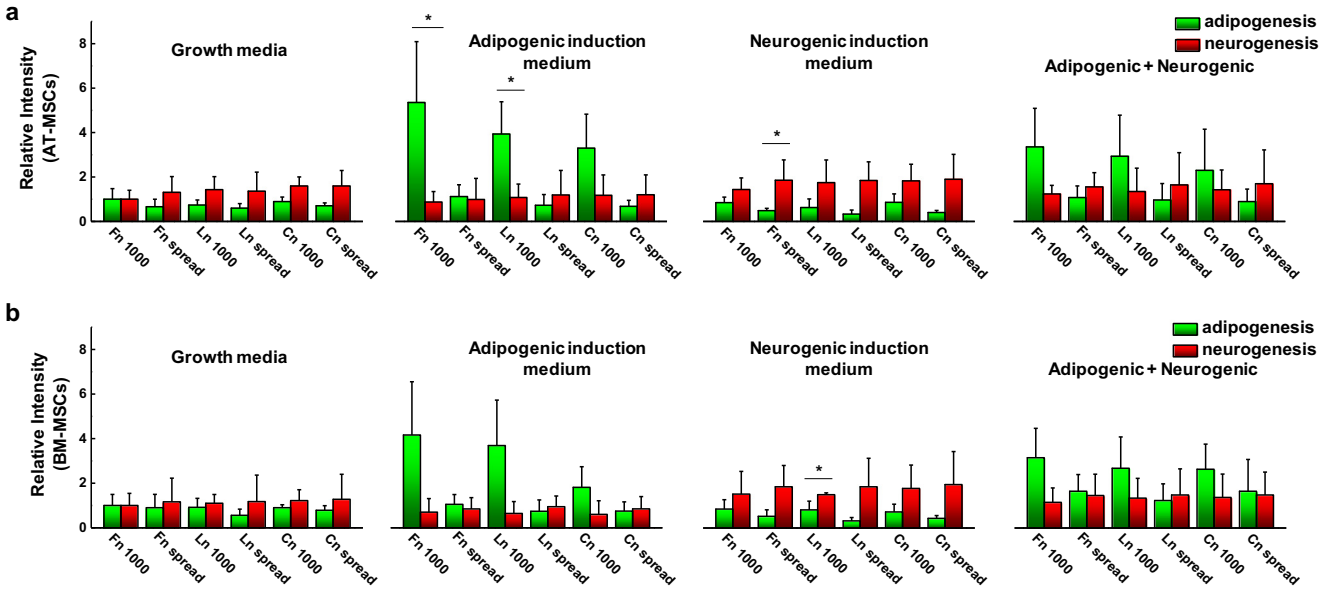

Fig. 3. MSCs express different levels of adipogenic and neurogenic markers with or without adipogenic/neurogenic induction media. Expression of adipogenic (PPAR- γ) and neurogenic (β3 tubulin) markers for (a) AT-MSCs and (b) BM-MSCs cultured for 10 days with or without adipogenic, neurogenic or combined induction medias while adherent to patterned (1000 μm^2) or non-patterned 0.5 kPa substrates coated with different matrix proteins (fibronectin, laminin, and collagen). (N = 3) (*P < 0.05, one-way ANOVA).

to BM-MSCs (Fig. 2f). Again, AT-MSCs appear to be more susceptible to changes in neurogenic marker expression and less susceptible to changes in PPAR γ expression compared to BM-MSCs [52].

To explore the influence of mixed induction media on differentiation, we compared PPAR γ and β3 tubulin expressions for AT- and BM-MSCs cultured in small circular shapes (1000 μm^2) or adherent to non-patterned surfaces of different matrix proteins on soft substrates (0.5 kPa) for 10 days with or without different combinations of induction media (Fig. 3). With only adipogenic induction medium, both AT- and BM-MSCs cultured in small circular patterns tend to express higher levels of PPAR γ (fibronectin > laminin > collagen), while those cultured on non-patterned substrates show no significant difference compared to growth medium except for those cultured on fibronectin. However, in neurogenic induction medium, β3 tubulin expression was elevated for both AT- and BM-MSCs cultured on both patterned and non-patterned substrates regardless of matrix proteins. When cultured with mixed (adipogenic + neurogenic) induction mediums, the trends are similar to those with only adipogenic induction media, but the adipogenic marker expression of AT- and BM-MSCs is lower, possibly due to the influence of neurogenic induction medium.

3.2. The role of cell shape and matrix protein in guiding AT- and BM-MSCs traction stress

Since AT- and BM-MSCs show dissimilar lineage outcomes in response to cell shape, stiffness, and protein composition, we hypothesized that MSCs from different sources may also exert variable traction force during differentiation [45]. First, we investigated focal adhesions in patterned AT- and BM-MSCs cultured for 1 or 10 days on different matrix proteins (fibronectin, laminin, and collagen); the results show similar expression of focal adhesion markers across different cell types and matrix proteins (Fig. S2). The traction stress exerted by AT- and BM-MSCs on small circle patterned or non-pattered hydrogels (0.5 kPa) across three different matrix proteins were measured (Fig. 4a) and visualized (Fig. 4b, insets are the cells via bright field microscopy before lysing). We observe that BM-MSCs on non-patterned substrates show higher traction stresses than those on small islands regardless of matrix proteins (9.1-fold on fibronectin; 2.1-fold on laminin; 1.4-fold on collagen). Traction exerted by AT-MSCs on laminin or collagen substrates showed no significant difference when comparing patterned and non-patterned cells while spread cells on fibronectin coated substrates displayed higher traction stress than those confined in small islands (17.9-fold on fibronectin). When comparing the same shape (patterned) across AT- and BM-MSCs, AT-MSCs showed slightly higher levels of traction stresses compared to BM-MSCs (~1.3-fold on fibronectin or collagen; ~1.5-fold on laminin). This may be in part because of the different sizes of AT- and BM-MSCs which will presumably influence the cells' ability to apply traction within the same adhesive area.

3.3. The expression of differentiation markers and integrin receptors for AT- and BM-MSCs on laminin coated substrates

Both patterned AT- and BM-MSCs show elevated expression of PPAR γ on fibronectin substrates, while those cultured on collagen coated matrices tend to express higher levels of β3 tubulin (Fig. S3a). However, when cultured on laminin substrates, AT-MSCs favored neurogenic specification, while BM-MSCs exhibit higher levels of adipogenic markers. Fig. 5a shows representative fluorescent images of AT- and BM-MSCs cultured on small islands conjugated with laminin. Percent differentiation shown in Fig. 5b

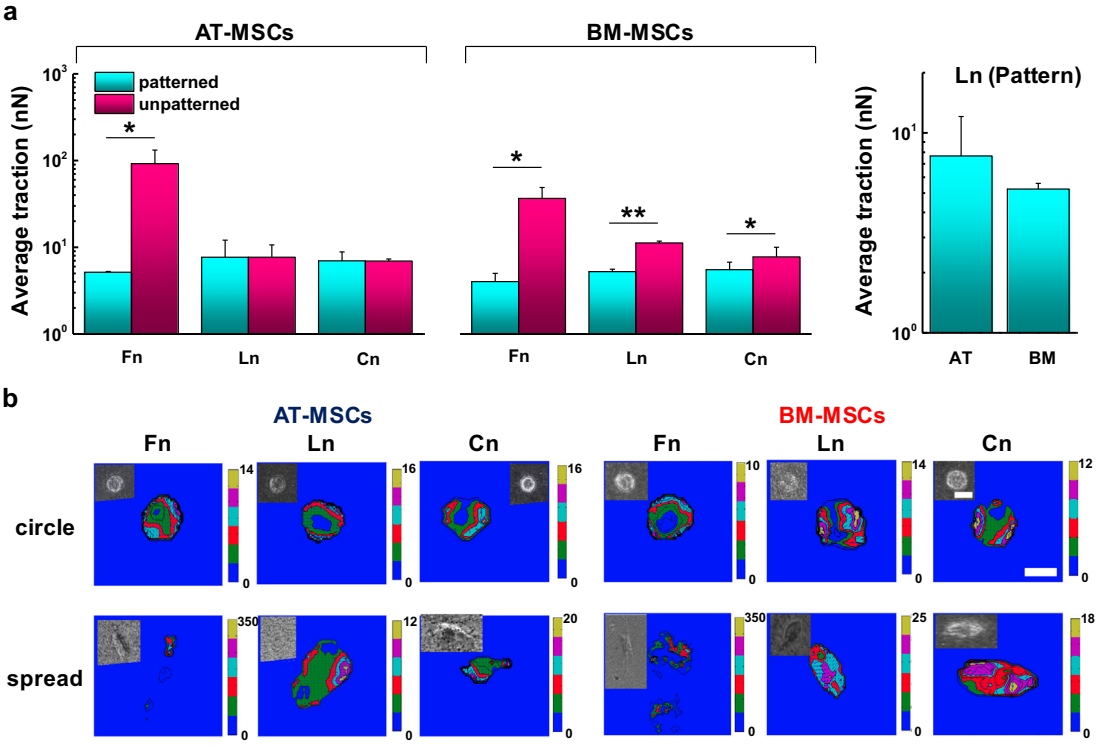

Fig. 4. Traction stress exerted by AT-MSCs and BM-MSCs is influenced by cell shape and matrix protein. (a) Average cellular traction stress for AT-MSCs and BM-MSCs cultured for 1 day on patterned (1000 μm^2) or non-patterned substrates coated with different matrix proteins (fibronectin, laminin, and collagen). (N = 3) (b) Representative traction map and phase-contrast image (inserted) of AT-MSCs and BM-MSCs cultured for 1 day with different biophysical and biochemical cues. Color bars at the right side of each traction stress map indicate stress value range in Pascal. Scale bar: 40 μm. (*P < 0.05 and **P < 0.005, one-way ANOVA). nN represents nanonewtons. Error bars represent s.d.

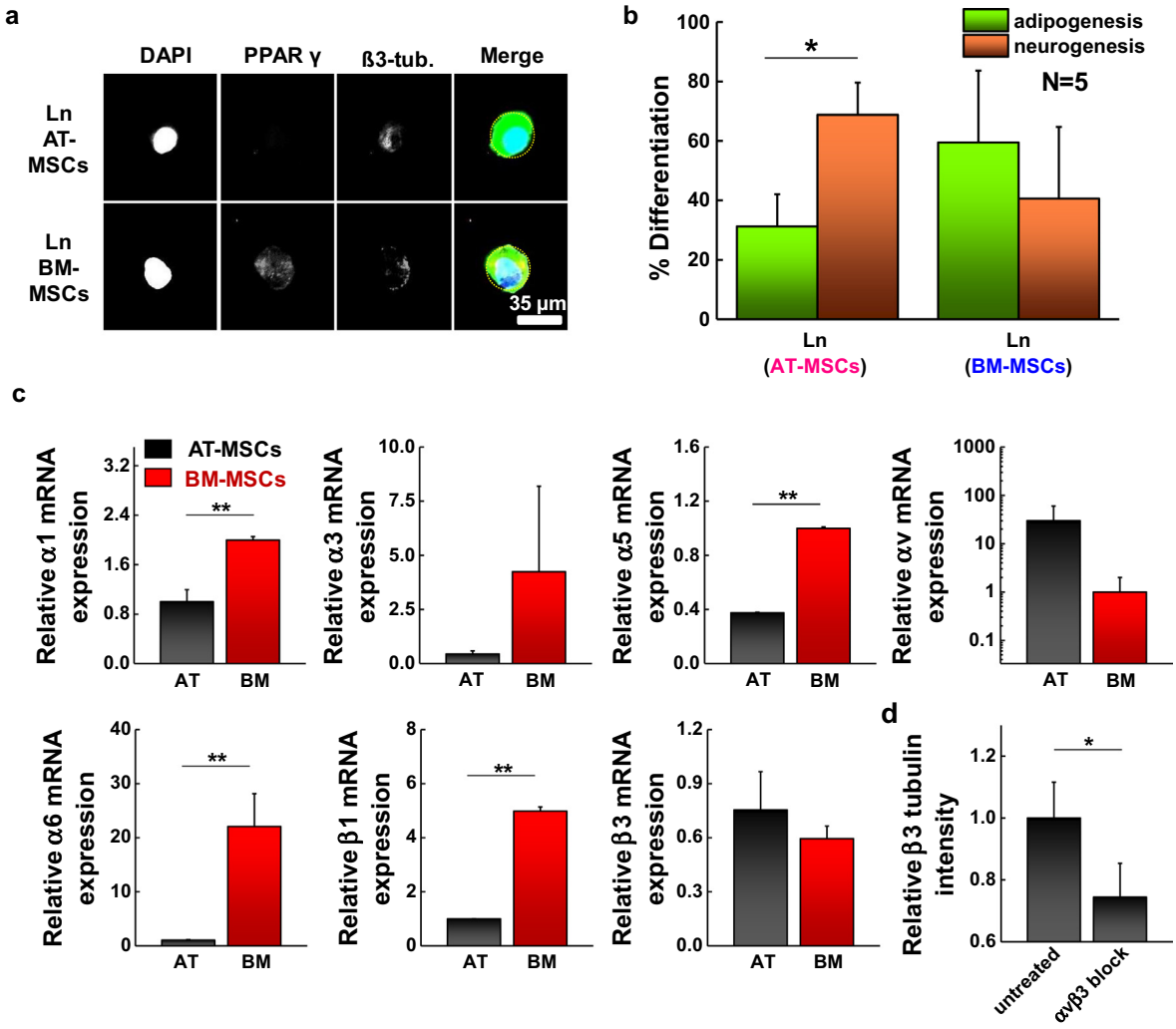

Fig. 5. Adhesion ligand (laminin) guides AT- and BM-MSC differentiation into different lineages with different integrin expression. (a) Representative immunofluorescence microscopy images of patterned AT-MSC and BM-MSC (1000 μm^2) cultured on a laminin coating and stained for PPAR γ and β3 tubulin. (b) Percentage of cells captured on small islands differentiating to adipocytic or neuronal lineages. (N = 3) (c) Results of real-time PCR to measure the gene expression of integrin α1, α3, α5, αv, α6, β1, and β3 of patterned AT-MSCs and BM-MSCs cultured for 1 day on laminin coated 0.5 kPa substrates. (N = 3) Expression of BM-MSCs compared to AT-MSCs (α1: 2.0-fold, α3: 9.6-fold, α5: 2.7-fold, αv: 0.03-fold, α6: 22.7-fold, β1: 5.0-fold, β3:0.77-fold) (d) Expression of β3 tubulin marker for AT-MSCs adherent to small circular shape of laminin patterned substrates with $\alpha_v\beta_3$ blocking. (N = 3) Immunofluorescence and flow cytometry results of integrin $\alpha_v\beta_3$ for AT- and BM-MSCs and marker expression of AT-MSCs and BM-MSCs cultured on small circles (laminin) with $\alpha_v\beta_3$ blocking are shown in Fig. S3 (*P < 0.05 and **P < 0.005, one-way ANOVA). Error bars represent s.d.

and S3b was obtained from intensity ratio via the comparisons with thresholds used to define lineage specification as previously reported [24]. AT-MSCs display higher expression levels of β3 tubulin with lower expression levels of PPAR γ, while BM-MSCs express both markers but with slightly higher levels of PPAR γ expression (Fig. 5b). To explore the role of integrin interactions of AT- and BM-MSCs on laminin in promoting different lineage specification, we analyzed the expression of various integrin receptors linked to laminin. Cells were cultured for 1 day on laminin patterned (1000 μm^2 circle) hydrogels (0.5 kPa) followed by RT-PCR of different integrin subunits. For most integrin receptors, BM-MSCs showed higher levels compared to AT-MSCs (2.0-fold α1; 9.6-fold α3; 2.7-fold α5; 22.7-fold α6; and 5.0-fold β1), however, AT-MSCs display higher expression for αv and β3 integrin (30.1-fold αv and 1.3-fold β3) (Fig. 5c). The trends in integrin expression are significantly different when MSCs are cultured on fibronectin or collagen (Fig. S4). Thus, we blocked $\alpha_v\beta_3$ using function blocking antibodies and measured the expression of PPAR γ and β3 tubulin. The results show that blocking integrin $\alpha_v\beta_3$ in AT-MSCs significantly decreased β3 tubulin expression compared to untreated cells (Fig. 5d), however the expression of PPAR γ for AT-MSCs and the expression of PPAR γ and β3 tubulin for BM-MSCs were not significantly changed (Fig. S5).

3.4. Reversibility of AT- and BM-MSC lineage specification by switching microenvironmental parameters

Previously, we showed that lineage specific markers display a degree of plasticity in BM-MSCs when transferred between different shapes or across matrices of different stiffness [53]. To explore the plasticity of AT- and BM-MSCs we first measured the expression of lineage specific markers under static conditions. Cells cultured for 10 days on small islands with fibronectin show elevated expression of PPAR γ (1.2-fold AT-MSCs and 1.7-fold BM-MSCs compared to those on non-patterned substrates) while cells cultured on non-patterned substrates tend to express elevated β3 tubulin levels (1.5-fold AT-MSCs and 1.2-fold BM-MSCs compared to those on patterned substrates) (Fig. 6). Next, cells were cultured for 5 days in patterned or non-patterned substrates and then transferred to non-patterned or patterned matrices, respectively,

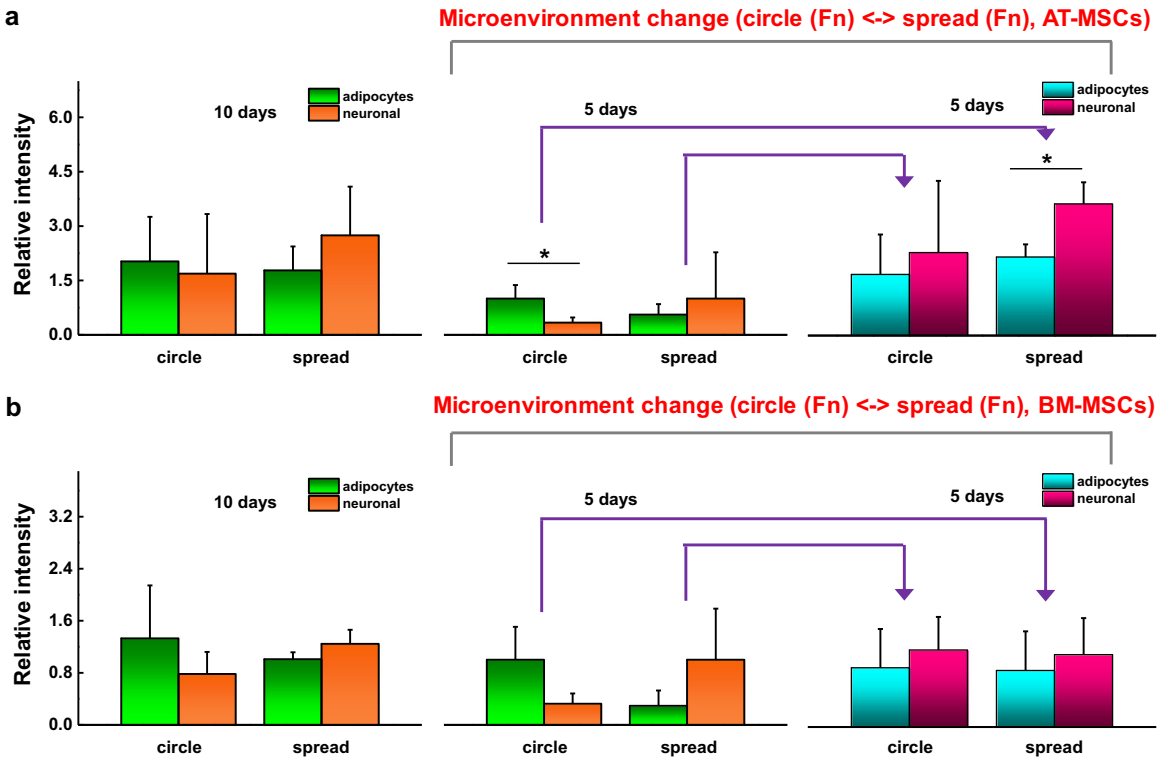

Fig. 6. Cell shape modulates the degree of MSC lineage specification. Expression of adipogenic (PPAR γ) and neurogenic (β3 tubulin) markers for (a) AT-MSCs and (b) BM-MSCs before and after switching the substrate after 10 days culture (patterned ⇔ non-patterned: cultured for 5 days in each original and switched substrate). (N = 3) (*P < 0.05, one-way ANOVA). Error bars represent s.d.

and re-cultured for 5 days. Both AT- and BM-MSCs (patterned to non-patterned) showed increased levels of the neurogenic marker (AT-MSCs: 2.3-fold PPAR γ and 6.5-fold β3 tubulin; BM-MSCs: 0.86-fold PPAR γ and 3.4-fold β3 tubulin). When cells were transferred from non-patterned to patterned substrates after 5 days, the expression of PPAR γ showed a further increase (AT-MSCs: 3.0-fold PPAR γ and 2.3-fold β3 tubulin; BM-MSCs: 3.1-fold PPAR γ and 1.2-fold β3 tubulin).

4. Discussion

Mesenchymal stem cells isolated from adipose tissue (AT-MSCs) and bone marrow (BM-MSCs) share similarities in general characteristics such as self-renewal, differentiation, and angiogenic potential [54]. However, there are several differences between AT- and BM-MSCs when comparing their specific characteristics. For instance, AT-MSCs have greater differentiation efficiency at higher passages compared to BM-MSCs [55]. Moreover, for in vitro differentiation, AT-MSCs have been shown to express higher levels of adipogenic markers [15,16,56], while BM-MSCs are more likely to differentiate down the osteogenic lineage path [17,18]. For example, during adipogenesis, AT-MSCs express higher levels of adipogenic lineage related genes than BM-MSCs including Lipoprotein lipase (LPL), Fatty acid-binding protein 4 (FABP4), Pyruvate Dehydrogenase Kinase, Isozyme 4 (PDK4), and Perilipins (PLIN) [56]. However, questions remain regarding how these cells from different sources respond to the biophysical and biochemical properties of the extracellular matrix. In this study we find that BM-MSCs show high spreading sensitivity to substrate stiffness, while cell spread area does not change as significantly for AT-MSCs as stiffness is increased. This corresponds to a decrease in adipogenesis for BM-MSCs with negligible or less significant changes in expression of adipogenic markers (PPAR γ or Nile red staining for lipid droplets) for AT-MSCs. Cells from both sources display decreased expression of β3 tubulin and MAP2 as stiffness is increased. This suggests adipogenesis in AT-MSCs is less sensitive to changes in bulk matrix elasticity, which may be related in part to cell spreading characteristics [24]. Previous studies have shown that the differentiation of BM-MSCs is regulated by not only matrix stiffness but also growth factors such as transforming growth factor β (TGF-β) [57–59]. For example, BM-MSCs can differentiate into smooth muscle cells (SMCs) on stiffer substrates and chondrogenic or adipogenic cells on soft substrates (~1 kPa), with TGF-β promoting increased expression of SMC and chondrogenic markers [57]. Here, we focus primarily on physical and biochemical factors influencing adipogenic and neurogenic differentiation for AT- and BM-MSCs. When stiffness, matrix composition and cell shape are normalized through micropatterning, AT-MSCs display relatively small changes in PPAR γ and a large increase in β3 tubulin expression as aspect ratio is increased. In contrast, BM-MSCs show a large decrease in PPAR γ expression and a modest increase in β3 tubulin. Taken together, these results suggest that the initial stages of adipogenesis and neurogenesis are regulated through matrix properties to different degrees depending on cell source.

Adhesion ligands can also influence MSC lineage specifications via the activation of different integrins [2,60]. For example, the expression of α5 and α6 integrin in BM-MSCs increase during osteogenesis and adipogenesis, respectively [2]. Consistent with our previous work [24], both AT- and BM-MSCs show a preference for adipogenesis when cultured on fibronectin and a preference for neurogenesis when cultured on collagen. However, when cultured on laminin, AT-MSCs favored a neurogenic outcome while BM-MSCs preferred an adipogenic outcome. Profiling the integrins involved in laminin adhesion reveals higher transcript expression of αv and β3 in AT-MSCs compared to BM-MSCs which show

significantly higher expression of α1, α5, α6 and β1. We speculate that the enhancement in expression of both αv and β3 integrin may be related to initiation of the neurogenesis program in AT-MSCs on laminin, and thus we blocked $\alpha_v\beta_3$ for cells cultured for 10 days on laminin conjugated small islands. Integrin $\alpha_v\beta_3$ has been implicated in osteogenesis of BM-MSCs cultured on fibronectin coated stiff substrates [45]; here $\alpha_v\beta_3$ integrin blocking leads to significantly lower levels of β3 tubulin, suggesting that neurogenesis may be facilitated by cellular sensing of laminin through integrin $\alpha_v\beta_3$.

In vitro, stem cell lineage is often guided through the use of soluble media supplements [61]. Thus, we employed adipogenic and neurogenic induction media, to explore how soluble cues guide differentiation under conditions of different matrix composition and mechanics. Both AT- and BM-MSCs cultured in small circular shapes or adherent to non-patterned surfaces of different matrix proteins on soft substrates for 10 days showed similar trends irrespective of media type. However, adipogenic induction media led to increased PPAR γ expression particularly for cells patterned on fibronectin matrices, while those cultured with neurogenic induction media showed elevated β3 tubulin levels irrespective of matrix protein and cell shape. When cells were exposed to a combination of induction cues, the trends were similar to adipogenic induction but with slight decreases in PPAR γ and increases in β3 tubulin expression. These results indicate that matrix parameters can set optimal initial conditions to guide lineage specification, with the addition of induction media serving to further promote differentiation. We employed traction force microscopy (TFM) to explore how the stress exerted on the substrate by AT- and BM-MSCs through specific integrin receptors may relate to lineage specification. Both AT- and BM-MSCs cultured on non-patterned fibronectin matrices were able to exert higher traction stress compared to cells cultured on laminin or collagen coated substrates. Interestingly, when confined to the same area through patterning the traction exerted by cells was slightly lower on fibronectin compared to laminin or collagen. In previous studies, MSCs which exert higher traction stress showed lower levels of adipogenic differentiation potential [47,48]. Consistent with these results, we see that the expression of markers associated with neurogenesis is maximized when matrix conditions favor spreading and the ability for a cell to exert traction. However, the composition of matrix and the integrins involved play a clear role in guiding these outcomes.

Previously we showed how switching the biophysical microenvironment, including stiffness and cell shape, could rewire lineage specification in BM-MSCs [53]. We speculated that cell spreading on soft substrates may play an important role in MSC neurogenesis. Thus we investigated switching the microenvironments between small circular patterned and non-patterned substrates to modulate adipogenesis and neurogenesis marker expression in AT- and BM-MSCs. The transfer of MSCs from patterned to non-patterned substrates led to increased β3 tubulin expression, while those transferred from non-patterned to patterned substrates maintained elevated β3 tubulin levels, suggesting a degree of irreversible activation once cells spread on the soft substrates.

Stem cell based therapy using cells from multiple sources is a promising strategy to treat a range of disorders including neurodegenerative disease, heart disease, and diabetes [62–64]. MSCs as a source of autologous cells have gained in popularity due to ease of isolation, and the capacity for differentiation across a variety of lineages including adipocytes, chondrocytes, myoblasts, osteoblasts, and neurocytes [65]. The integration of soft biomaterials with MSCs requires an understanding of the biophysical and biochemical basis underlying specification and commitment to a desired lineage [66]. The results of the present study provide insight into the role of cell shape, matrix stiffness and protein composition in guiding lineage specification for MSCs from different sources.

5. Conclusion

In this study, we show how the adipogenic and neurogenic differentiation potential of AT- and BM-MSCs can be influenced by controlling matrix stiffness, cell shape, and the composition of adhesion protein. AT- and BM-MSCs' expression of adipogenic and neurogenic markers is guided differently by the properties of the extracellular matrix: AT-MSCs are more sensitive to their environment in regards to neurogenic marker expression, while BM-MSCs are more sensitive to their environments in regards to adipogenic marker expression. In particular, AT- and BM-MSCs on small islands with laminin coated soft substrates show distinct lineage outcomes: neurogenesis of AT-MSCs and adipogenesis of BM-MSCs. Integrin profiling and traction force measurements on laminin conjugated soft gels suggest AT-MSCs initiate neurogenic signaling through $\alpha_v\beta_3$-mediated adhesion. This work suggests that MSCs from different sources have different susceptibilities for extracellular guidance of lineage, which highlights the importance of cell and matrix selection for the intended application.

Disclosures

The authors indicate no potential conflicts of interest.

Acknowledgments

This work was supported by the National Heart Lung and Blood Institute of the National Institutes of Health, Grant number HL121757.

Appendix A. Supplementary data

Supplementary data associated with this article can be found, in the online version, at http://dx.doi.org/10.1016/j.actbio.2016.06.037.

References

[1] W.L. Murphy, T.C. Mcdevitt, A.J. Engler, Materials as stem cell regulators, Nat. Mater. 13 (2014) 547–557.
[2] J.E. Frith, R.J. Mills, J.E. Hudson, J.J. Cooper-White, Tailored integrin-extracellular matrix interactions to direct human mesenchymal stem cell differentiation, Stem Cells Dev. 21 (2012) 2442–2456.
[3] S. Lv, D.M. Dudek, Y. Cao, M.M. Balamurali, J. Gosline, H. Li, Designed biomaterials to mimic the mechanical properties of muscles, Nature 465 (2010) 69–73.
[4] Y. Shao, J. Sang, J. Fu, On human pluripotent stem cell control: The rise of 3D bioengineering and mechanobiology, Biomaterials 52 (2015) 26–43.
[5] Y. Li, K.A. Kilian, Bridging the Gap: From 2D cell culture to 3D microengineered extracellular matrices, Adv. Healthc. Mater. (2015) 2780–2796.
[6] M. Al-Nbaheen, R. Vishnubalaji, D. Ali, A. Bouslimi, F. Al-Jassir, M. Megges, A. Prigione, J. Adjaye, M. Kassem, A. Aldahmash, Human stromal (mesenchymal) stem cells from bone marrow, adipose tissue and skin exhibit differences in molecular phenotype and differentiation potential, Stem Cell Rev. Rep. 9 (2013) 32–43.
[7] D.A. De Ugarte, K. Morizono, A. Elbarbary, Z. Alfonso, P.A. Zuk, M. Zhu, J.L. Dragoo, P. Ashjian, B. Thomas, P. Benhaim, I. Chen, J. Fraser, M.H. Hedrick, Comparison of multi-lineage cells from human adipose tissue and bone marrow, Cells Tissues Organs 174 (2003) 101–109.
[8] S. Kern, H. Eichler, J. Stoeve, H. Klüter, K. Bieback, Comparative analysis of mesenchymal stem cells from bone marrow, umbilical cord blood, or adipose tissue, Stem Cells 24 (2006) 1294–1301.
[9] P.A. Zuk, M. Zhu, P. Ashjian, D.A.D. Ugarte, J.I. Huang, H. Mizuno, Z.C. Alfonso, J. K. Fraser, P. Benhaim, M.H. Hedrick, Prosper Benhaim, human adipose tissue is a source of multipotent stem cells, Mol. Biol. Cell. 13 (2002) 4279–4295.
[10] M. Dominici, K. Le Blanc, I. Mueller, I. Slaper-Cortenbach, F. Marini, D. Krause, R. Deans, A. Keating, D.J. Prockop, E. Horwitz, Minimal criteria for defining multipotent mesenchymal stromal cells. The International Society for Cellular Therapy position statement, Cytotherapy 8 (2006) 315–317.
[11] S. Gronthos, D.M. Franklin, H.A. Leddy, P.G. Robey, R.W. Storms, J.M. Gimble, Surface protein characterization of human adipose tissue-derived stromal cells, J. Cell. Physiol. 189 (2001) 54–63.
[12] F. Festy, L. Hoareau, S. Bes-Houtmann, A.-M. Péquin, M.P. Gonthier, A. Munstun, J.J. Hoarau, M. Cesari, R. Roche, Surface protein expression between human adipose tissue-derived stromal cells and mature adipocytes, Histochem, Cell Biol. 124 (2005) 113–121.

[13] Y.A. Romanov, A.N. Darevskaya, N.V. Merzlikina, L.B. Buravkova, Mesenchymal stem cells from human bone marrow and adipose tissue: isolation, characterization, and differentiation potentialities, Bull. Exp. Biol. Med. 140 (2005) 138–143.
[14] R.A. Panepucci, J.L.C. Siufi, W.A. Silva, R. Proto-Siquiera, L. Neder, M. Orellana, V. Rocha, D.T. Covas, M.A. Zago, Comparison of gene expression of umbilical cord vein and bone marrow-derived mesenchymal stem cells, Stem Cells. 22 (2004) 1263–1278.
[15] G. Pachón-Peña, G. Yu, A. Tucker, X. Wu, J. Vendrell, B.A. Bunnell, J.M. Gimble, Stromal stem cells from adipose tissue and bone marrow of age-matched female donors display distinct immunophenotypic profiles, J. Cell. Physiol. 226 (2011) 843–851.
[16] Y. Sakaguchi, I. Sekiya, K. Yagishita, T. Muneta, Comparison of human stem cells derived from various mesenchymal tissues: superiority of synovium as a cell source, Arthritis Rheum. 52 (2005) 2521–2529.
[17] I. Bochev, G. Elmadjian, D. Kyurkchiev, L. Tzvetanov, I. Altankova, P. Tivchev, S. Kyurkchiev, Mesenchymal stem cells from human bone marrow or adipose tissue differently modulate mitogen-stimulated B-cell immunoglobulin production in vitro, Cell Biol. Int. 32 (2008) 384–393.
[18] D. Noël, D. Caton, S. Roche, C. Bony, S. Lehmann, L. Casteilla, C. Jorgensen, B. Cousin, Cell specific differences between human adipose-derived and mesenchymal-stromal cells despite similar differentiation potentials, Exp. Cell Res. 314 (2008) 1575–1584.
[19] R.H. Lee, B. Kim, I. Choi, H. Kim, H.S. Choi, K. Suh, Y.C. Bae, J.S. Jung, Characterization and expression analysis of mesenchymal stem cells from human bone marrow and adipose tissue, Cell Physiol. Biochem. 14 (2004) 311–324.
[20] A.J. Engler, S. Sen, H.L. Sweeney, D.E. Discher, Matrix elasticity directs stem cell lineage specification, Cell 126 (2006) 677–689.
[21] M. Krampera, S. Marconi, A. Pasini, M. Galiè, G. Rigotti, F. Mosna, M. Rinelli, L. Lovato, E. Anghileri, A. Andreini, G. Pizzolo, A. Sbarbati, B. Bonetti, Induction of neural-like differentiation in human mesenchymal stem cells derived from bone marrow, fat, spleen and thymus, Bone 40 (2007) 382–390.
[22] G.C. Reilly, A.J. Engler, Intrinsic extracellular matrix properties regulate stem cell differentiation, J. Biomech. 43 (2010) 55–62.
[23] K.A. Kilian, B. Bugarija, B.T. Lahn, M. Mrksich, Geometric cues for directing the differentiation of mesenchymal stem cells, Proc. Natl. Acad. Sci. USA 107 (2010) 4872–4877.
[24] J. Lee, A.A. Abdeen, D. Zhang, K.A. Kilian, Directing stem cell fate on hydrogel substrates by controlling cell geometry, matrix mechanics and adhesion ligand composition, Biomaterials 34 (2013) 8140–8148.
[25] K. Ye, X. Wang, L. Cao, S. Li, Z. Li, L. Yu, J. Ding, Matrix stiffness and nanoscale spatial organization of cell-adhesive ligands direct stem cell fate, Nano Lett. 15 (2015) 4720–4729.
[26] K.A. Kilian, M. Mrksich, Directing stem cell fate by controlling the affinity and density of ligand-receptor interactions at the biomaterials interface, Angew. Chem. Int. Ed. Engl. 51 (2012) 4891–4895.
[27] J. Lee, A.A. Abdeen, A.S. Kim, K.A. Kilian, Influence of biophysical parameters on maintaining the mesenchymal stem cell phenotype, ACS Biomater. Sci. Eng. 1 (2015) 218–226.
[28] A.G. Cristancho, M.A. Lazar, Forming functional fat: a growing understanding of adipocyte differentiation, Nat. Rev. Mol. Cell Biol. 12 (2011) 722–734.
[29] W.S. Choi, M. Kim, S. Park, S.K. Lee, T. Kim, Patterning and transferring hydrogel-encapsulated bacterial cells for quantitative analysis of synthetically engineered genetic circuits, Biomaterials 33 (2012) 624–633.
[30] R. Peng, X. Yao, J. Ding, Effect of cell anisotropy on differentiation of stem cells on micropatterned surfaces through the controlled single cell adhesion, Biomaterials 32 (2011) 8048–8057.
[31] S. Wislet-Gendebien, G. Hans, P. Leprince, J.M. Rigo, G. Moonen, B. Rogister, Plasticity of cultured mesenchymal stem cells: switch from nestin-positive to excitable neuron-like phenotype, Stem Cells. 23 (2005) 392–402.
[32] P. Lu, A. Blesch, M.H. Tuszynski, Induction of bone marrow stromal cells to neurons: differentiation, transdifferentiation, or artifact?, J Neurosci. Res. 77 (2004) 174–191.
[33] J. Lyahyai, D.R. Mediano, B. Ranera, A. Sanz, A.R. Remacha, R. Bolea, P. Zaragoza, C. Rodellar, I. Martin-Burriel, Isolation and characterization of ovine mesenchymal stem cells derived from peripheral blood, BMC Vet. Res. 8 (2012) 169.
[34] Y. Jiang, D. Henderson, M. Blackstad, A. Chen, R.F. Miller, C.M. Verfaillie, Neuroectodermal differentiation from mouse multipotent adult progenitor cells, Proc. Natl. Acad. Sci. USA 100 (Suppl 1) (2003) 11854–11860.
[35] M.K.X. Long, M. Olszewski, W. Huang, Neural cell differentiation in vitro from adult human bone marrow mesenchymal stem cells, Stem Cells Dev. 14 (2005) 65–69.
[36] D.L. Jones, A.J. Wagers, No place like home: anatomy and function of the stem cell niche, Nat. Rev. Mol. Cell Biol. 9 (2008) 11–21.
[37] Y.K. Wang, C.S. Chen, Cell adhesion and mechanical stimulation in the regulation of mesenchymal stem cell differentiation, J. Cell. Mol. Med. 17 (2013) 823–832.
[38] F. Guilak, D.M. Cohen, B.T. Estes, J.M. Gimble, W. Liedtke, C.S. Chen, Control of stem cell fate by physical interactions with the extracellular matrix, Cell Stem Cell 5 (2009) 17–26.
[39] X. Yao, R. Peng, J. Ding, Cell-material interactions revealed via material techniques of surface patterning, Adv. Mater. 25 (2013) 5257–5286.
[40] S. Mitragotri, J. Lahann, Physical approaches to biomaterial design, Nat. Mater. 8 (2009) 15–23.
[41] C. Huang, J. Dai, X.A. Zhang, Environmental physical cues determine the lineage specification of mesenchymal stem cells, Biochim. Biophys. Acta 2015 (1850) 1261–1266.
[42] S. Gronthos, P.J. Simmons, S.E. Graves, P.G. Robey, Integrin-mediated interactions between human bone marrow stromal precursor cells and the extracellular matrix, Bone 28 (2001) 174–181.
[43] R.O. Hynes, Integrins: versatility, modulation, and signaling in cell adhesion, Cell 69 (1992) 11–25.
[44] J.D. Humphries, A. Byron, M.J. Humphries, Integrin ligands at a glance, J. Cell Sci. 119 (2006) 3901–3903.
[45] J. Lee, A.A. Abdeen, X. Tang, T.A. Saif, K.A. Kilian, Biomaterials Geometric guidance of integrin mediated traction stress during stem cell differentiation, Biomaterials 69 (2015) 174–183.
[46] N. Wang, J.P.P. Butler, D.E.E. Ingber, Mechanotransduction across the cell surface and through the cytoskeleton, Science 260 (1993) 1124–1127.
[47] S. Khetan, M. Guvendiren, W.R. Legant, D.M. Cohen, C.S. Chen, J.A. Burdick, Degradation-mediated cellular traction directs stem cell fate in covalently crosslinked three-dimensional hydrogels, Nat. Mater. 12 (2013) 458–465.
[48] J. Fu, Y.K. Wang, M.T. Yang, R.A. Desai, X. Yu, Z. Liu, C.S. Chen, Mechanical regulation of cell function with geometrically modulated elastomeric substrates, Nat. Methods 7 (2010) 733–736.
[49] J.R. Tse, A.J. Engler, Preparation of hydrogel substrates with tunable mechanical properties, Curr. Protoc. Cell Biol. 47 (2010). 10.16.1–10.16.16.
[50] J. Lee, A.A. Abdeen, T.H. Huang, K.A. Kilian, Controlling cell geometry on substrates of variable stiffness can tune the degree of osteogenesis in human mesenchymal stem cells, J. Mech. Behav. Biomed. Mater. 209–218 (2014).
[51] X. Tang, A. Tofangchi, S.V. Anand, T.A. Saif, A novel cell traction force microscopy to study multi-cellular system, PLoS Comput. Biol. 10 (2014) e1003631.
[52] M. Pevsner-Fischer, S. Levin, D. Zipori, The origins of mesenchymal stromal cell heterogeneity, Stem Cell Rev. Rep. 7 (2011) 560–568.
[53] J. Lee, A.A. Abdeen, K.A. Kilian, Rewiring mesenchymal stem cell lineage specification by switching the biophysical microenvironment, Sci. Rep. 4 (2014) 5188.
[54] M. Strioga, S. Viswanathan, A. Darinskas, O. Slaby, J. Michalek, Same or not the same? Comparison of adipose tissue-derived versus bone marrow-derived mesenchymal stem and stromal cells, Stem Cells Dev. 21 (2012) 2724–2752.
[55] R. Izadpanah, C. Trygg, B. Patel, C. Kriedt, J. Dufour, J.M. Gimble, B.A. Bunnell, Biologic properties of mesenchymal stem cells derived from bone marrow and adipose tissue, J. Cell. Biochem. 99 (2006) 1285–1297.
[56] T.M. Liu, M. Martina, D.W. Hutmacher, J.H. Hui, E.H. Lee, B. Lim, Identification of Common Pathways mediating differentiation of bone marrow- and adipose tissue-derived human mesenchymal stem cells into three mesenchymal lineages, Stem Cells. 25 (2007) 750–760.
[57] J.S. Park, J.S. Chu, A.D. Tsou, R. Diop, Z. Tang, A. Wang, S. Li, The effect of matrix stiffness on the differentiation of mesenchymal stem cells in response to TGF-β, Biomaterials 32 (2011) 3921–3930.
[58] D. Wang, J.S. Park, J.S.F. Chu, A. Krakowski, K. Luo, D.J. Chen, S. Li, Proteomic profiling of bone marrow mesenchymal stem cells upon transforming growth factor ß 1 stimulation, J. Biol. Chem. 279 (2004) 43725–43734.
[59] E.J. Williams CG, T.K. Kim, A. Taboas, A. Malik, P. Manson, In vitro chondrogenesis of bone marrow-derived mesenchymal progenitor cells, Tissue Eng. 9 (2003) 679–688.
[60] A.S. Rowlands, P.A. George, J.J. Cooper-White, Directing osteogenic and myogenic differentiation of MSCs: interplay of stiffness and adhesive ligand presentation, Am. J. Physiol. 295 (2008) C1037–C1044.
[61] C. Vater, P. Kasten, M. Stiehler, Culture media for the differentiation of mesenchymal stromal cells, Acta Biomater. 7 (2011) 463–477.
[62] S. Ding, P.G. Schultz, A role for chemistry in stem cell biology, Nat. Biotechnol. 22 (2004) 833–840.
[63] D. Karussis, I. Kassis, B.G.S. Kurkalli, S. Slavin, Immunomodulation and neuroprotection with mesenchymal bone marrow stem cells (MSCs): a proposed treatment for multiple sclerosis and other neuroimmunological/neurodegenerative diseases, J. Neurol. Sci. 265 (2008) 131–135.
[64] M.E. Bernardo, D. Pagliara, F. Locatelli, Mesenchymal stromal cell therapy: a revolution in regenerative medicine?, Bone Marrow Transplant 47 (2012) 164–171.
[65] D. Baksh, L. Song, R.S. Tuan, Adult mesenchymal stem cells: characterization, differentiation, and application in cell and gene therapy, J. Cell. Mol. Med. 8 (2004) 301–316.
[66] M.P. Lutolf, J.A. Hubbell, Synthetic biomaterials as instructive extracellular microenvironments for morphogenesis in tissue engineering, Nat. Biotechnol. 23 (2005) 47–55.